

**APPLICATION OF REMOTE SENSING AND FRACTAL MODELING IN IDENTIFYING THE ALTERATION ZONES IN MUTEH COMPLEX- CENTRAL IRAN****APLICAÇÃO DE SENSORIAMENTO REMOTO E MODELAGEM FRACTAL NA IDENTIFICAÇÃO DE ZONAS DE ALTERAÇÃO NO COMPLEXO DE MUTEH - IRÃ CENTRAL**Nasim Zamani<sup>1</sup>Mohammad Lotfi\*<sup>2</sup>Mohsen Pourkermani<sup>3</sup>**ABSTRACT**

Muteh complex is located in the Northeast of the Golpayegan city and in the middle part of Sanandaj-Sirjan metamorphic complex. The host rock is mostly Schist and Gneisses, that are intruded and altered by younger granitic units. Gold mineralization is attributed to pyritic materials in host rock, that after leaching and destruction into Fe-hydroxides under the process of Alunitization, the gold related materials would be released and its grade in the altered rock units grows up. Three types of pyrite are present in the samples. The first generation of pyrite is parallel to the host rock schistosity. The second generation is perpendicular to the host rock schistosity and third generation is in fractures. Structurally high grade of the Au has accorded in places where conjugated faults with northwest to southeast trend are presents. The alteration type of area was identified by Spectral Angle Mapper(SAM) method and then have been classified by Number-Size(N-S) fractal method: also conjugate faults were extracted by using ETM+ satellite images and then classified by Concentration- Area fractal method. the most parts of altered areas and gold mineralization related to these conjugated faults; XRD analysis, confirm the remote sensing method results and fire assay analysis is used for determining gold concentration in these areas.

**Keywords:** Muteh complex; Alunite and Jarosite mineralization; Spectral Angle Mapper (SAM) method, Number-Size (N-S) fractal method; Fire assay analysis.

**RESUMO**

O complexo Muteh está localizado no nordeste da cidade de Golpayegan e na parte central do complexo metamórfico Sanandaj-Sirjan. A rocha hospedeira é principalmente xisto e

<sup>1</sup>Department of Geology, North Tehran branch, Islamic Azad University, Tehran, Iran. [zamanis72@yahoo.com](mailto:zamanis72@yahoo.com)  
ORCID: <https://orcid.org/0000-0001-5825-284X>

<sup>2</sup>Geological survey of Iran, Tehran, Iran. \*Corresponding author. [mlofti20@yahoo.com](mailto:mlofti20@yahoo.com) ORCID:  
<http://orcid.org/0000-0002-5414-1381>

<sup>3</sup>Department of Geology, North Tehran branch, Islamic Azad University, Tehran.  
[Iranmohsen.pourkermani@gmail.com](mailto:Iranmohsen.pourkermani@gmail.com) ORCID: <http://orcid.org/0000-0003-3445-760X>

gnaisse, que são intrometidos e alterados por unidades graníticas mais jovens. A mineralização do ouro é atribuída aos materiais piríticos nas rochas hospedeiras, que após a lixiviação e a destruição dos hidróxidos de Fe sob o processo de alunização, os materiais relacionados ao ouro seriam liberados e seu grau nas unidades de rochas alteradas aumentaria. Três tipos de pirita estão presentes nas amostras. A primeira geração de pirita é paralela à esquistose da rocha hospedeira. A segunda geração é perpendicular à esquistose da rocha hospedeira e a terceira geração está em fraturas. Estruturalmente, o alto grau da Au é concedido em locais onde estão presentes falhas conjugadas com tendência noroeste a sudeste. O tipo de alteração da área foi identificado pelo método Spectral Angle Mapper (SAM) e, em seguida, foi classificado pelo método fractal Número-Tamanho (N-S): também foram extraídas falhas conjugadas usando imagens de satélite ETM + e depois classificadas pelo método fractal Concentração-Área. a maior parte das áreas alteradas e a mineralização de ouro relacionadas a essas falhas conjugadas; A análise de DRX, confirma os resultados do método de sensoriamento remoto e a análise de ensaio de incêndio é usada para determinar a concentração de ouro nessas áreas.

**Palavras-Chave:** Complexo de Muteh; Mineração de alunita e jarosita; Método de Mapeamento de Ângulo Espectral (SAM); Método fractal Número-Tamanho (N-S). Análise de fogo.

## INTRODUCTION

Muteh complex is located in northeast of 1:250000 geological sheet of Golpayegan and district is located in the central part of the Sanandaj-Sirjan metamorphosed zone of the Zagros orogenic belt (Figure 1). There are nine gold deposits and occurrences in the Muteh mining district (Figure 2). The study area is in Chah khatun mine that consists of two parts: eastern and western (Figure 3). The gold mineralization is accord in the zones that are deformed due to the three deformation stages (D1-D3), of which D2 is the most important phase forming a WNW-trending (N280-N290°), reverse, dextral, ductile shear zone by 3 km long and 2 km wide; also the hydrothermal alterations accorded in the inner parts of wall rocks (Kuhestani *et al.*, 2015; Nazemi *et al.*, 2019). The intensity of alterations is variable and ranges from weak to pervasive. Silicification and Sulfidation of wall rocks are usually observed in the western parts in altered shear zones (Kuhestani *et al.*, 2015). In the eastern part, high sulfide minerals such as pyrite decay due to forming the Iron oxide mineral Such as alunite and jarosite. this part is brown, because gold is in the pyritic network and after

pyrite destruction, it releases and the grade is upgrade, so they can recognize by multi-spectral satellite data depends on the wavelength range and power of spectral separation of their sensors. The spectral domain of the short wave infrared (SWIR) as a part of the electromagnetic wavelength is one of the important tools for detection of argillic, phyllic and propylitic alteration zones (Abrams *et al.*, 1983; Rutz-Armenta, Prol-Ledesma, 1998; Sabins, 1999; Tangestani, Moore 2001; Sadeghi *et al.*, 2013; Aramesh *et al.*, 2015; Yazdi *et al.*, 2019a, 2019b; Jamshidibadr *et al.*, 2020). In this paper, Remote sensing and the Spectral Angle Mapper (SAM) method has been used, to recognize the Iron oxide mineralization which results from pyrite decay such as alunite and jarosite, and then were separated by Number-Size fractal model to find their abundance and classify them.

### **REGIONAL GEOLOGY**

The Sanandaj-Sirjan Zone is a NW-SE trending belt of mainly metamorphic and igneous rocks, located at the northeastern extension of the Zagros Orogeny (Figure 1). To the northeast, it is bordered by Central Iran and the UDMA, and to the southwest by the Zagros Fold Thrust belt (Alavi, 2004). The Sanandaj-Sirjan Zone consists mainly of Late Proterozoic–Mesozoic metamorphic rocks, such as metacarbonates, schists, gneisses, and amphibolites (Figure 2). They are overlain by Phanerozoic shallow-water sediments of a passive continental margin and intruded by large gabbroic to granitic Mesozoic plutons (Dilek *et al.*, 2010). Similar geological characteristics suggest a westward extension of the Sanandaj-Sirjan Zone into the BitlisPuturge Zone in Turkey (Dilek *et al.*, 2010). Both of these zones consist of Precambrian crystalline basement, Late Proterozoic–Mesozoic metacarbonates, schist, gneiss, and amphibolite's that are intruded upon by deformed to undeformed granitoid plutons. U-Pb dating of detrital zircons of Phanerozoic sedimentary rocks from several localities across Iran and the presence of inherited zircons in younger intrusions indicate, that the bulk of the crystalline basement of Iran.

### **GEOLOGICAL SETTING**

Muteh gold deposit, is characterized by having a high-grade metamorphic core (mainly gneiss and amphibolite) covered by low-grade metamorphic rocks (mainly green schist, metarhyolite and marble). Chlorite schist is the predominant host rock in Muteh gold district. Mesozoic and Tertiary sedimentary rocks overlaying Paleozoic sedimentary rocks, are abundant in the study area, and quaternary alluvial sediments covered them in a large quantity (Figure 5). The metamorphic complex is intruded by middle to late cretaceous and paleocene-eocene granitic plutons (Moritz *et al.*, 2006). Gold mineralization is related to a protracted geologic evolution of the Sanandaj-Sirjan tectonic zone and magmatic-metamorphic hydrothermal activity (Moritz, 2006). Mineralization is similar to mesothermal quartz vein type deposits in orogenic belts and is controlled by brittle, ductile to ductile–brittle shear zones. Hydrothermal alteration associated with gold occurrences is characterised by intense, pervasive bleaching of the host rocks (Moritz *et al.*, 2006). Alteration assemblages consist of silicified rock with microcrystalline to crystalline quartz, fine-grained muscovite, pyrite, dolomite-ankerite, and albite overprinting the metamorphic minerals in the host rock (Moritz *et al.*, 2006). Pyritization is the dominant alteration and is rather extensive and related to gold mineralization (Abdollahi *et al.*, 2009; Dabiri *et al.*, 2018; Baratian *et al.*, 2018; Daya, 2019; Novruzov *et al.*, 2019). Gold paragenetic minerals include principal sulphide phases as pyrite, arsenopyrite and chalcopyrite. Three types of pyrite are present in the samples. the first generation of pyrite is parallel to the host rock schistosity. the second generation is perpendicular to the host rock schistosity and third generation is in younger fractures. (Figure 4)

There are no visible gold grains and gold commonly occurs as very fine-grained solid inclusions (1–5  $\mu\text{m}$ ) in pyrite and arsenopyrite (Keshavarzi *et al.*, 2012).

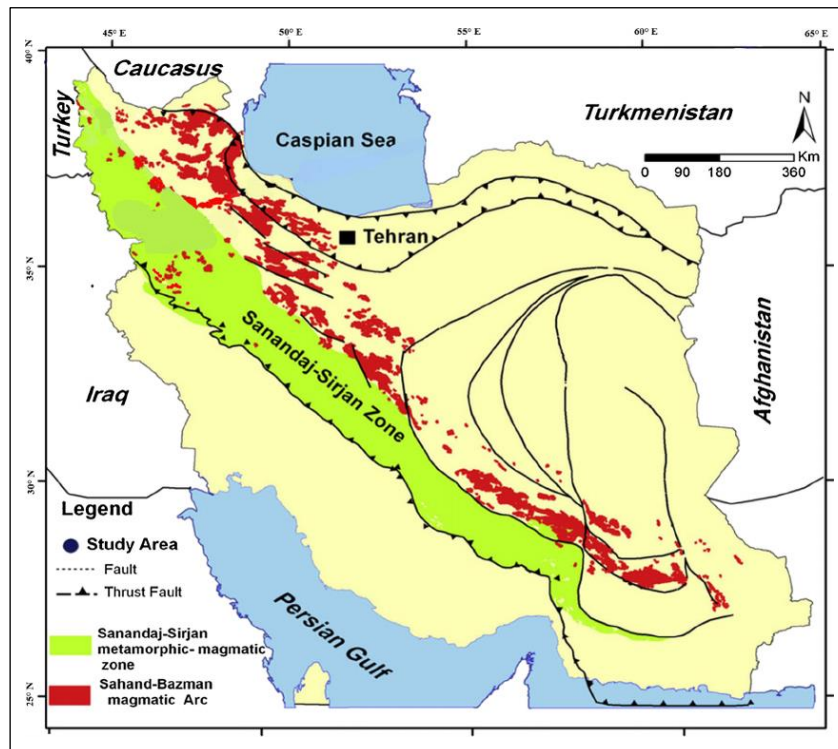


Figure 1. Location of study area in the Sanandaj – Sirjan zone which was accomplished and simplified.  
Source: Based on the 1:1000,000 geologic map of Iran by Sahandi et al. (2005).

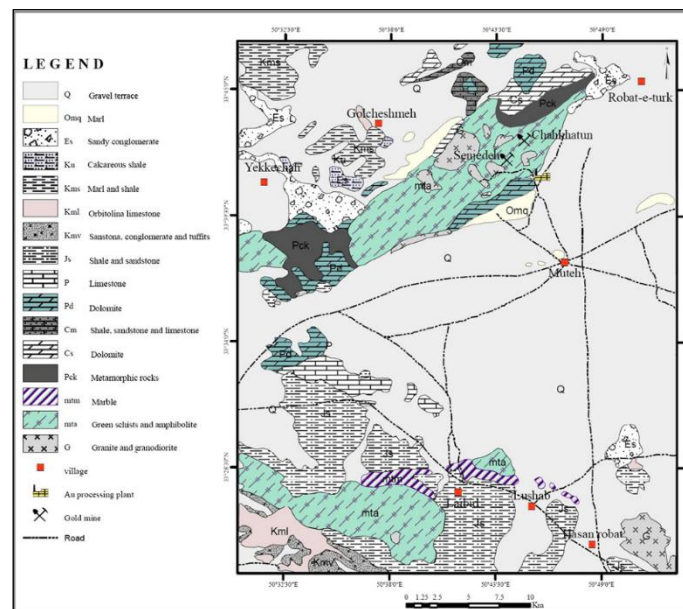


Figure 2. Simplified geological map of Muteh district.  
Keshavarzi et al. (2012).



Figure 3. Overview of (a) eastern and (b) western parts of (c) Chah Khatun mine.  
Source: Zamani *et al.*(2020).

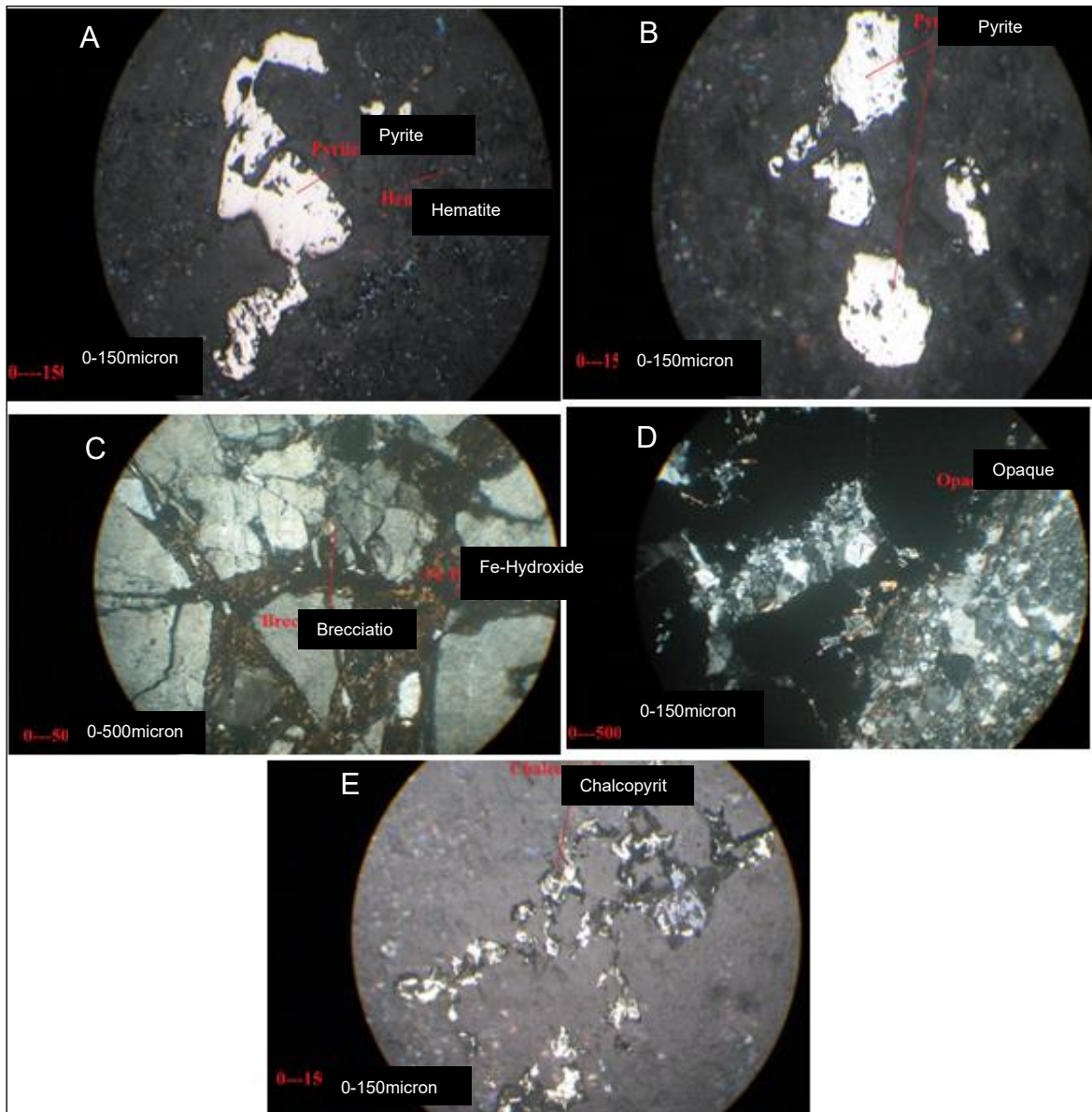


Figure 4. (a) (b) first generation of pyrite; (c) (d) second generation of pyrite; (e) third generation of sulfide in Chah Khatun mine.

Source: Zamani *et al.*(2020).

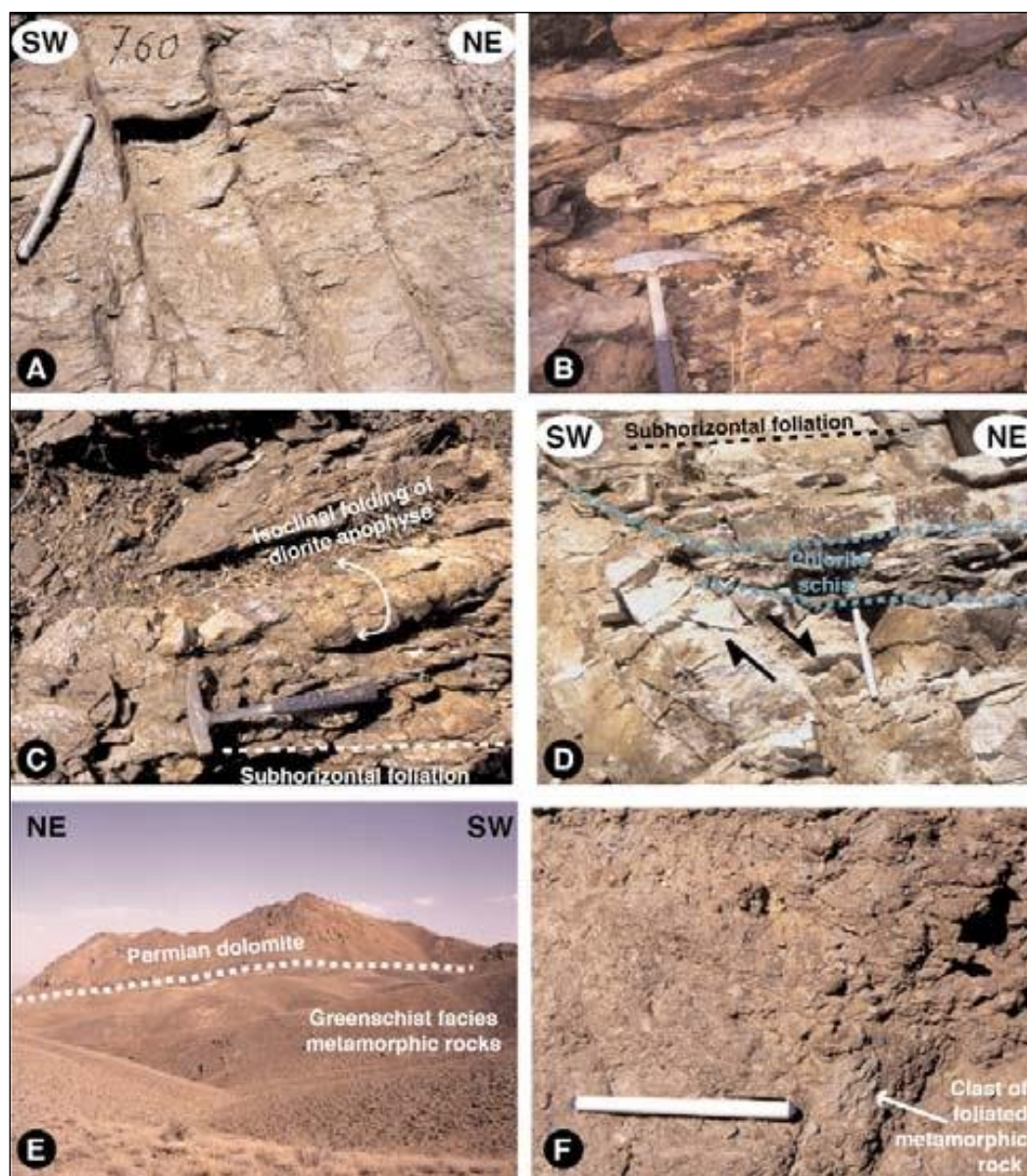


Figure 5. Geological status of the area  
Source: Moritz *et al.* (2006).

## METHODOLOGY

In this research, the areas that are containing the alunite and jarosite mineralization, recognized by Spectral Angle Mapper (SAM) method and the area of each mineralized zone have been calculated, then these localities were classified with Number-Size fractal model and the altered zone for both alunite and jarosite mineral have been defined. This zones have been checked by field observation and mineralography studies and XRD method.

### SPECTRAL ANGLE MAPPER (SAM) CLASSIFIER

The SAM method is applied by many researchers in remote sensing studies for mineral exploration (Kruse *et al.*, 1993; Tangestani *et al.*, 2008). It is a physically-based spectral classification that uses an n-dimensional angle to match pixels to reference spectra. The algorithm determines the spectral similarity between the image and reference spectra by calculating and comparing the cosine value of these two spectra. High cosine values between the two spectra indicate high similarity, whereas low values indicate low similarity (Abdoli Sereshgi *et al.*, 2019). The cosine value can be computed using an equation (1), where nb, ti and ri are number of bands, reflectance of band i for image spectrum, and reflectance of band i for reference spectrum, respectively as follows (Fakhari *et al.*, 2019):

$$\cos \alpha = \frac{\sum_{i=1}^{nb} t_i r_i}{\sqrt{\sum_{i=1}^{nb} t_i^2} \sqrt{\sum_{i=1}^{nb} r_i^2}}$$

### NUMBER-SIZE FRACTAL MODEL

The N-S model proposed has been expressed as follows:

$$N(\geq \rho) = C\rho^{-D}$$

Where  $\rho$  is the average size of the blasted rocks,  $N(\rho)$  is the number of samples with equal  $\rho$ , C is a constant and D is the fractal dimension. The model shows that there is a relationship between desired features (average size of the blasted rocks) and the cumulative number of samples. The log-log plots of  $N(\rho)$  versus  $\rho$  show the scattered data points which can then be fitted by several straight lines (segments) with different slopes based on a least-square regression (Afzal *et al.*, 2012). The selection of breakpoints as threshold values seems to be an objective decision since fragmented rocks populations are addressed by different line segments in the N-S log-log plots. As a result, the intensity of various populations is depicted by each slope of the line segment in the N-S log-log plots (Nikzad *et al.* 2018).

## APPLICATION OF SAM METHOD IN RECOGNITION OF MINERALS IN MUTEH COMPLEX

SAM method used to recognition two different type of Iron oxide mineralization, alunite and jarosite, which are related to gold mineralization. For this purpose, the spectrum of were extracted from the ENVI spectral library (Figure 6) and then the spectral map of each of them was prepared. The SAM method shows the big concentration of alunite and jarosite in the middle and south east parts of the study area (Figure 7). Finally, the size of each mineralized part was calculated and data extracted to calculation by fractal modeling.

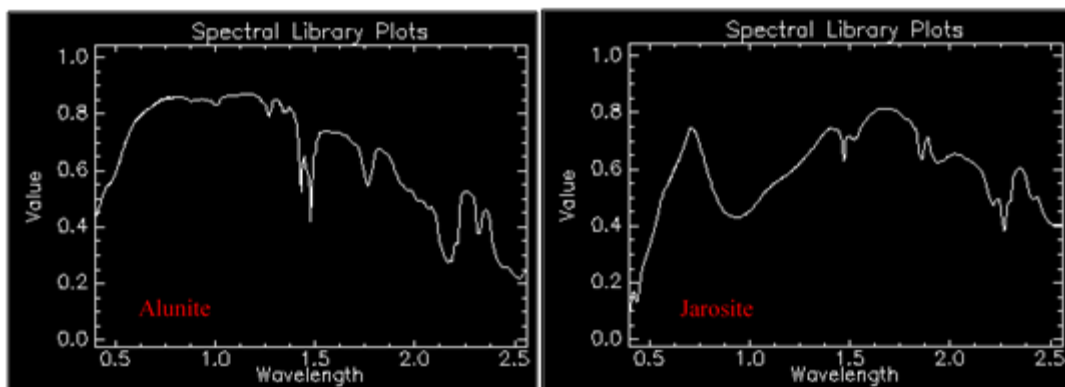


Figure 6. Spectral plots of Alunite and Jarosite extracted from Envi spectral library file.

Source: Zamani *et al.*(2020).

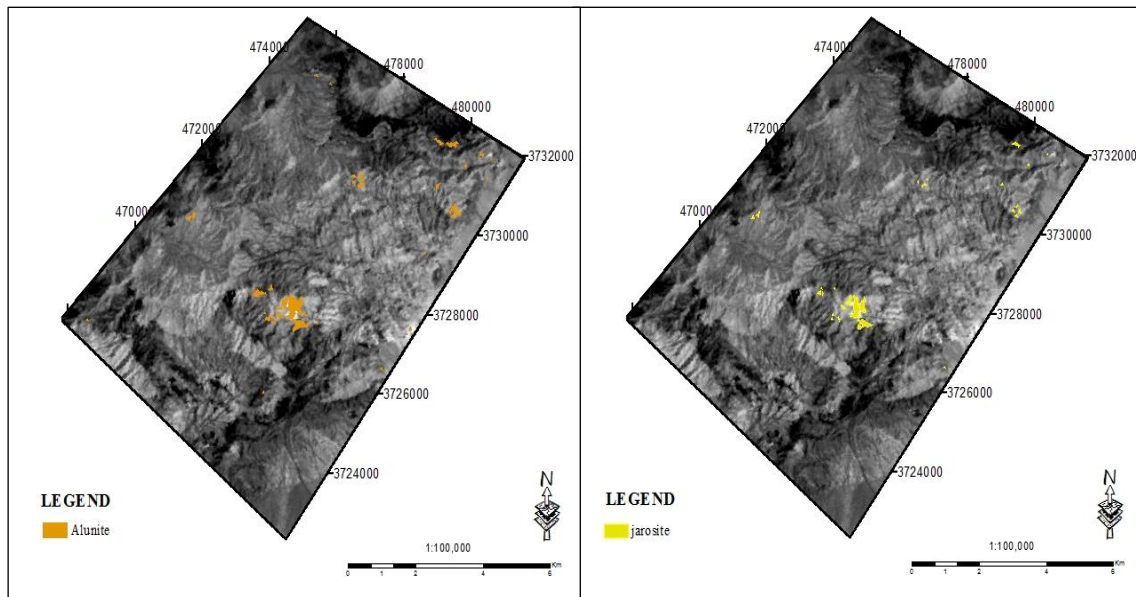


Figure 7. The spectral map of the Alunite and Jarosite in Muteh complex enhanced by SAM method  
Source: Zamani *et al.* (2020).

#### APPLICATION OF N-S FRACTAL MODEL

Two N-S log-log plots have been illustrated with respect to satellite images processing using SAM method' and analysis of them for each one of alunite and jarosite mineralization zone and threshold values were determined for the mineralization areas. The N-S log-log plots reveal, that there are five populations for the both alunite and jarosite mineralization. For alunite the populations range start from the 18 Km<sup>2</sup> and the high area is 1393 Km<sup>2</sup> and for jarosite these amounts are start from the 43 Km<sup>2</sup> to 1393 Km<sup>2</sup> (Figure 8 and 9). Table 1 shows the amount of each population that divided by N-S fractal model.

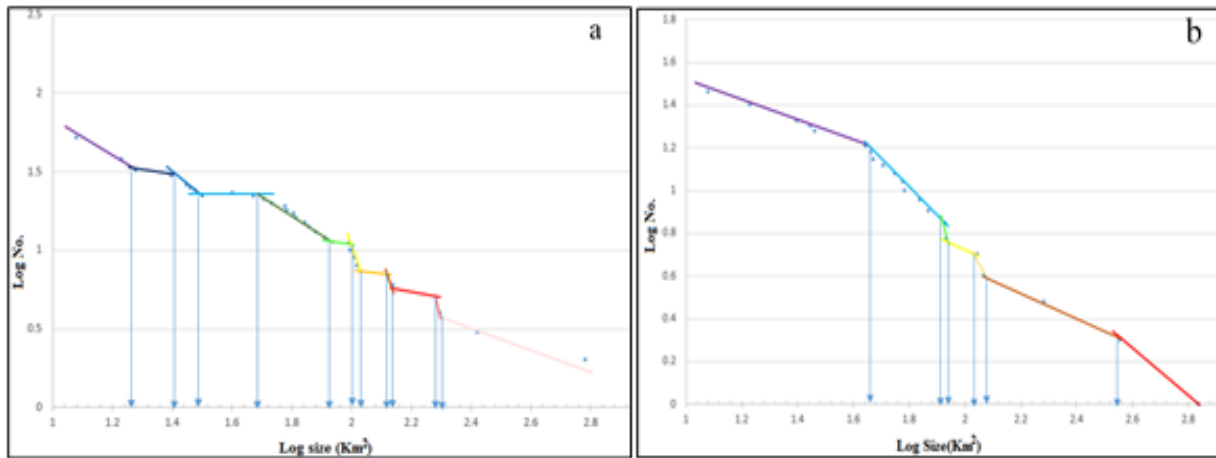


Figure 8. N-S fractal log-log plots for the alunite (a); and jarosite (b) in Muteh area. Source: Zamani et al.(2020).

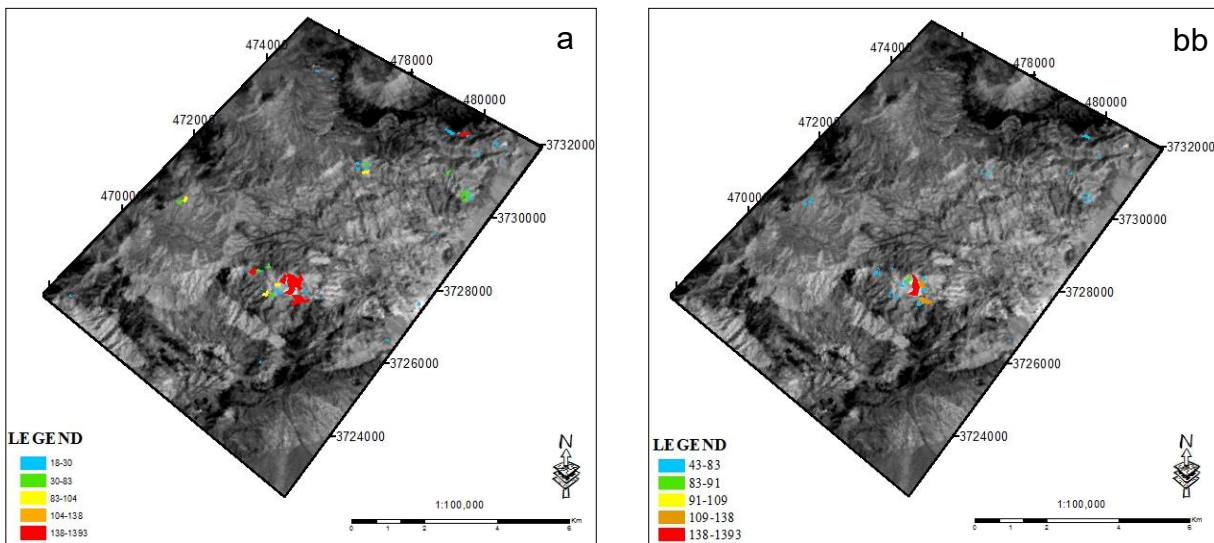


Figure 9. N-S Model for the alunite (a); and jarosite (b) in Muteh area. Source: Zamani et al.(2020).

Mineral	The first population	The second population	The third population	The forth population	The fifth population
Alunite	18-30	30-83	83-104	104-138	138-1393
Jarosite	43-83	83-91	91-109	109-138	138-1393

Table 1. The statistical community of alunite and jarosite mineralization Source: Zamani et al.(2020).

This model shows the high extent of the alunite and jarosite mineralization is concentrated in central parts of the study area, these parts have the highest rate of the leaching and could be rich in gold.

### CORRELATION BETWEEN RESULTS OF FRACTAL MODELING AND GEOLOGICAL PARTICULARS

#### RESULTS OF (XRD) METHOD IN SURVEYING MUTEH SAMPLES

XRD is the key tool in mineral exploration. Mineralogists have been among the foremost in developing and promoting the new field of X-ray crystallography after its discovery. Thus, the advent of XRD has literally revolutionized the geological sciences to such a degree that they have become unthinkable without this tool. Nowadays, any geological group actively involved in mineralogical studies would be lost without XRD to unambiguously characterize individual crystal structures. Each mineral type is defined by a characteristic crystal structure, which will give a unique X-ray diffraction pattern, allowing rapid identification of minerals present within a rock or soil sample. The XRD data can be analyzed to determine the proportion of the different minerals present. In this research the results of the remote sensing studies and fractal modeling verified by XRD results (Bunaciu et al 2015). So, the parts of study area that was identified as the target area were sampling (Figure 10) and four rock samples have been taken to (XRD) analyzing). These studies have been carried out to determine the presence of minerals and gold in these samples (Figure 11).

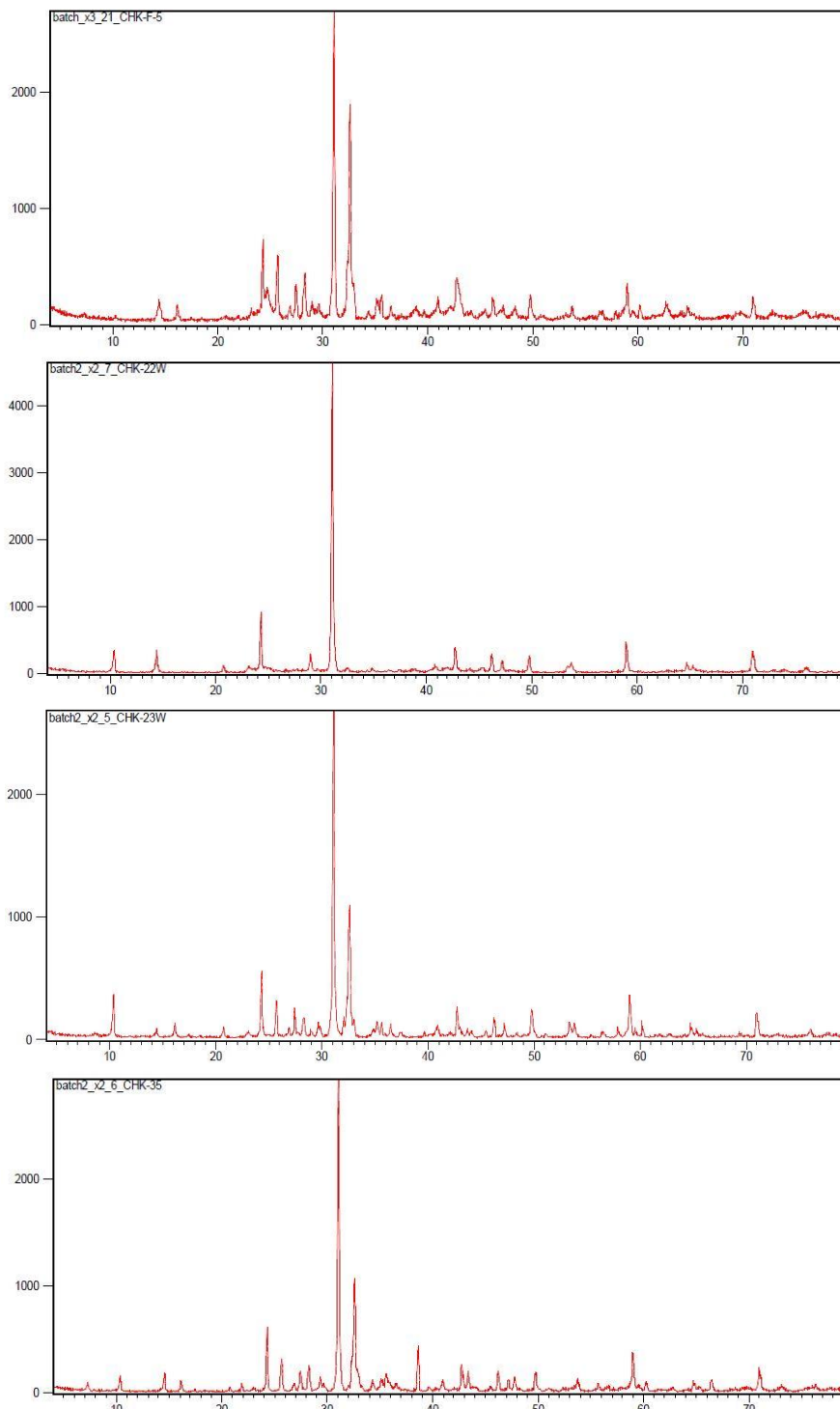


Figure 10. XRD graphs of samples taken from altered zones.  
Source: zamani *et al.*(2020).

Sample ID.	Minerals
CHK-F-5	Si O <sub>2</sub> ; Quartz; Na ( Al Si <sub>3</sub> O <sub>8</sub> ); Albite low ;Al <sub>2</sub> ( Si <sub>2</sub> O <sub>5</sub> ) ( O H ) <sub>4</sub> ; Kaolinite ;( Mg , Al , Fe ) <sub>6</sub> ( Si , Al ) <sub>4</sub> O <sub>10</sub> ( O H ) <sub>8</sub> ; Clinocllore K Al <sub>3</sub> Si <sub>3</sub> O <sub>10</sub> ( O H ) <sub>2</sub> ; Muscovite
CHK-23W	Si O <sub>2</sub> ; Quartz, Na ( Al Si <sub>3</sub> O <sub>8</sub> ); Albite; K Al <sub>2</sub> ( Si <sub>3</sub> Al ) O <sub>10</sub> ( O H , F ) <sub>2</sub> ; Muscovite; Al <sub>2</sub> Si <sub>2</sub> O <sub>5</sub> ( O H ) <sub>4</sub> ; Kaolinite; K Si <sub>3</sub> Al O <sub>8</sub> ; Orthoclase; ( K , H <sub>3</sub> O ) Al <sub>2</sub> Si <sub>3</sub> Al O <sub>10</sub> ( O H ) <sub>2</sub> ; Illite
CHK-35	Si O <sub>2</sub> ; Quartz; Fe S <sub>2</sub> ; Pyrite ;Na ( Al Si <sub>3</sub> O <sub>8</sub> ); Albite ( Mg , Fe ) <sub>6</sub> ( Si , Al ) <sub>4</sub> O <sub>10</sub> ( O H ) <sub>8</sub> ; Clinocllore ;Ca ( C O <sub>3</sub> ); Calcite ;K Al <sub>2</sub> ( Si <sub>3</sub> Al ) O <sub>10</sub> ( O H , F ) <sub>2</sub> ; Muscovite
CHK-22W	SiO <sub>2</sub> ; Quartz; H <sub>2</sub> K Al <sub>3</sub> ( Si O <sub>4</sub> ) <sub>3</sub> ; Muscovite; Al <sub>2</sub> ( Si <sub>2</sub> O <sub>5</sub> ) ( O H ) <sub>4</sub> ; Kaolinite; K Al <sub>3</sub> Si <sub>3</sub> O <sub>10</sub> ( O H ) <sub>2</sub> ; Muscovite; Fe +3 O ( O H ); Goethite

Table 2. Minerals detected by XRD method from samples taken from altered areas.

Source: zamani et al.(2020).



Figure 10. The altered zone (alunite, jarosite and silica) in Muteh complex

Source: Zamani et al.(2020).

### MINERALOGRAPHIC STUDIES

Mineralogical studies have been performed on Muteh Complex samples for accurately detecting and separating alterations under the microscope and also determining the relationship of gold mineralization with major alterations in the areas which determined by remote sensing; these studies were separated alunite and jarosite, silice and gold mineralization that was observed in the thin-polished sections (Figure 11).

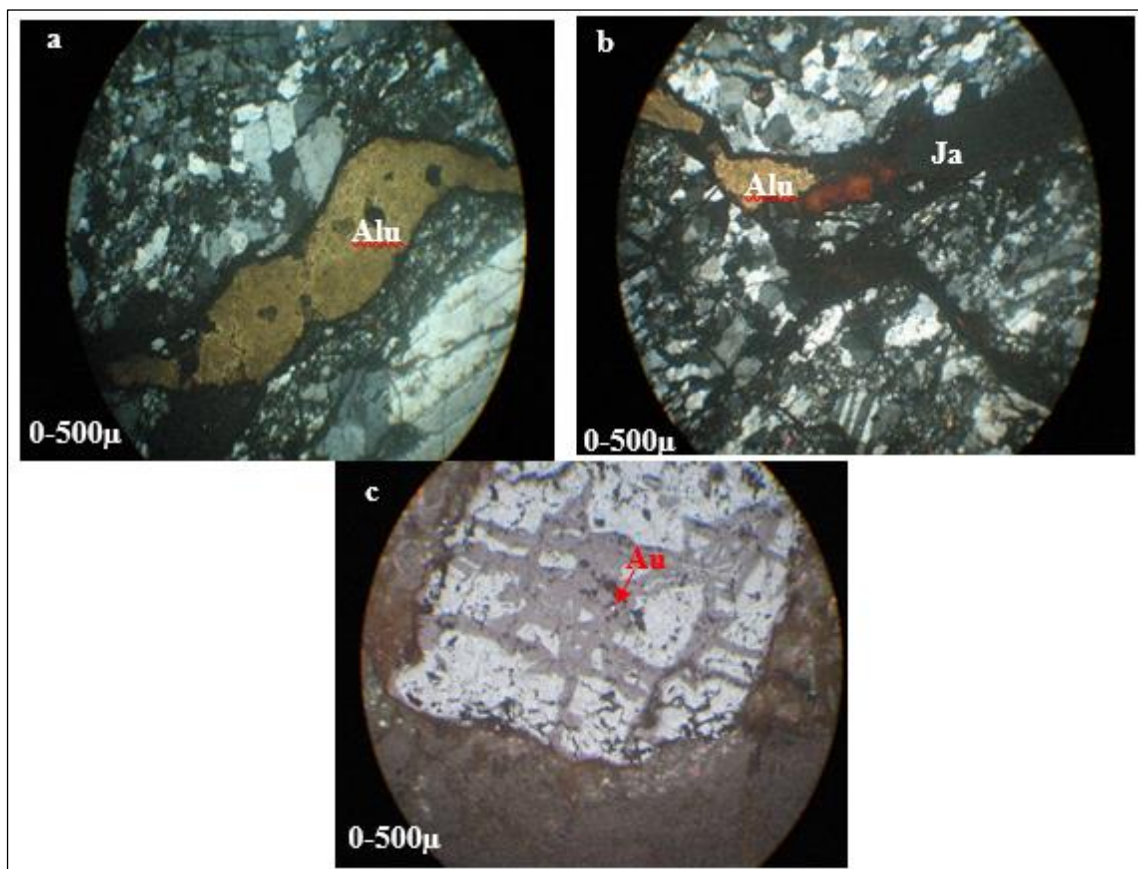


Figure 11. (a) alunite; (b) jarosite and alunite; (c) gold mineralization in thin-polished sections.

Source: Zamani *et al.*(2020).

### **CONCLUSION**

Study the minerals that are related to the gold mineralization, alunitization, jarositization and also the results of the remote sensing studies by SAM method, shows the high amount of mineralization in central and eastern parts of the study area. These results were processed by N-S fractal modeling and identified the places that had a great and less

extent of the alunite and jarosite and they were separated; also the extent of the alunite in the central parts of the study area is greater than jarosite which, this shows the range of the alunite is more than jarosite in the Muteh mine. At the end, the thin –polish sections that provided to mineralogical study shows, the correlation between the gold mineralization, alunite and jarosite in this area .

## REFERENCES

- ABDOLI SERESHGI, H.; GANJI, A.; ASHJA ARDALAN, A.; TORSHIZIAN, H.; TAHERI, J. Detection of metallic prospects using staged factor and fractal analysis in Zouzan region, NE Iran, **Iranian Journal of Earth Sciences**, 11(4), 2019. p. 256-266.
- ABDOLLAHI, M. J.; KARIMPOUR, M. H.; KHERADMAND, A.; ZARASVANDI, A. R. Stable Isotopes (O, H, and S) in the Muteh Gold Deposit, Golpaygan Area, Iran, **Natural Resources Research**, 18, 2009. p. 137–151.
- ABRAMS, M. J.; BROWN, D.; LEPLEY, L.; SADOWSKI, R. Remote sensing for porphyry copper deposits in southern Arizona. **Economic Geology** 78(4), 1983. p. 591-604.
- AFZAL, P.; FADAKAR ALGHALANDIS, Y.; MOAREFVAND, P.; RASHIDNEJAD OMRAN, N.; ASADI, H. Application of power-spectrum–volume fractal method for detecting hypogene, supergene enrichment, leached and barren zones in Kahang porphyry Cu deposit, Central Iran. **Journal of Geochemical Exploration**, n. 112, 2012. p. 131-138.
- ALAVI, M. Regional Stratigraphy of the Zagros Fold-Thrust Belt of Iran and its Evolution. **American Journal of Science**, 304, 2004.p.43-47
- ARAMESH, A. S. L. R.; AFZAL, P.; ADIB, A.; YASREBI, A. Application of multifractal modeling for the identification of alteration zones and major faults based on ETM+ multispectral data. **Journal of the Indian Society of Remote Sensing**, 43(1),2015. p. 121–132.
- BARATIAN, M.; ARIAN, M. A.; YAZDI, A. Petrology and petrogenesis of the Siah Kuh intrusive Massif in the South of Khosh Yeilagh, **Amazonia Investiga**, 7(7), 2018. p. 616-629.
- DABIRI, R.; AKBARI-MOGADDAM, M.; GHAFARI, M. Geochemical evolution and petrogenesis of the eocene Kashmar granitoid rocks, NE Iran: implications for fractional crystallization and crustal contamination processes. **Iranian Journal of Earth Sciences**, 10(1), 2018. p. 68-77.
- DAYA, A. A. Nonlinear disjunctive kriging for the estimating and modeling of a vein copper deposit. **Iranian Journal of Earth Sciences**, 11(3), 2019. p. 226-236.
- DILEK, Y.; IMAMVERDIYEV, N.; ALTUNKAYNAK, S. Geochemistry and tectonics of Cenozoic volcanism in the Lesser Caucasus (Azerbaijan) and the peri-Arabian region, collision-induced mantle dynamics and its magmatic fingerprint. **International Geology Review**, 152, 2010. p. 536–578.
- FAKHARI, S.; JAFARIRAD, A.; AFZAL, P.; LOFTI, M. Delineation of hydrothermal alteration zones for porphyry systems utilizing ASTER data in Jebel-Barez area, SE Iran. **Iranian Journal of Earth Sciences** ,11(1) 2019. p. 80-92.

- JAMSHIDIBADR, M.; TARABI, S.; GHOLIZADEH, K. Study of micro-textures and chemistry of feldspar minerals of East Sarbisheh volcanic complex (Eastern Iran), for evidence of magma chamber process. **Iranian Journal of Earth Sciences**, 12(1) 2020. p. 10-31.
- KESHAVARZI, B.; MOORE, F.; RASTMANESH, F.; JAFARKHANI, M. Arsenic in the Muteh gold mining district, Isfahan, Iran. **Environmental Earth Sciences**, 67,4, 2012. p.777-786
- KOUHESTANI, H.; CHANG, Z.; JOHNSON, A.; MOKHTARI, A.; STEIN, J. Timing and genesis of ore formation in the Qarachilar Cu-Mo-Au deposit, Ahar-Arasbaran metallogenic zone, NW Iran, Evidence from geology, fluid Inclusions-S isotope and Re-Os geochronology, **Elsevier ore geology reviews**, 102, 2015. p. 757-775.
- KRUSE, F. A.; LEFKOFF, A.; BOARDMAN, J. W.; HEIDEBRECHT, K. B.; SHAPIRO, A. T.; BARLOON, J. P. The spectral image processing system (SIPS) - Interactive visualization and analyses of imaging spectrometer data. **Remote Sensing of Environment**, 44, 1993. p. 145-163.
- MORITZ, R.; GHAZBAN, F.; SINGER, B. S. Eocene gold ore formation at Muteh, Sanandaj-Sirjan Tectonic Zone, Western Iran, a result of late-stage extension and exhumation of metamorphic basement rocks within the Zagros Orogen. **Economic Geology**, 2006. p. 101, p. 1497–1524.
- NAZEMI, E.; ARIAN, M. A.; JAFARIAN, A. POURKERMANI, M.; YAZDI, A. Studying The Genesis Of Igneous Rocks In Zarin-Kamar Region (Shahrood, Northeastern Iran) By Rare Earth Elements. **Revista Gênero e Direito**, 8(4), 2019. p. 446-466.
- NIKZAD, M.; ASADI, A.; YASREBI, A.; WETHERELT, A.; AFZAL, P. Blast fragmentation classification using number-size (N-S) fractal model in Jalal-abad iron mine. **Archives of Mining Sciences**, 63. 2018. p. 783-796. DOI: <10.24425/123697>.
- NOVRUZOV, N.; VALIYEV, A.; BAYRAMOV, A.; MAMMADOV, S.; IBRAHIMOV, J.; EBDULREHIMLI, A. Mineral composition and paragenesis of altered and mineralized zones in the Gadir low sulfidation epithermal deposit (Lesser Caucasus, Azerbaijan). **Iranian Journal of Earth Sciences**, 11(1), 2019. p. 14-29.
- RUTZ-ARMENTA, J. R.; PROL-LEDESMA, R. M. Techniques for enhancing the spectral response of Hydrothermal alteration minerals in thematic mapper images of central Mexico. **Journal Remote Sensing**, 19, 1998. p. 1981–2000.
- SABINS, F. F. Remote Sensing for Mineral Exploration. **Ore Geology Reviews**, 14, 1999. p. 157-183.
- SADEGHI, B.; KHALAJMASOUMI, M.; AFZAL, P.; MOAREFVAND, P.; YASREBI, A. B.; WETHERELT, A.; FOSTER, P.; ZIAZARIFI, A. Using ETM+ and ASTER sensors to identify iron occurrences in the Esfordi 1: 100,000 mapping sheet of Central Iran. **Journal of African Earth Sciences**, 103 (114), 2013. p. 103-114
- TANGESTANI, M. H.; MOORE, F. Comparison of three principal component analyses techniques to porphyry copper alteration mapping, a case study in Meiduk area, Kerman, Iran, Can J, **Remote Sensing**, 27, 2001. p. 176–182.
- YAZDI, A.; ASHJA ARDALAN, A.; EMAMI, M. H.; DABIRI, R.; FOUDAZI, M. () Magmatic interactions as recorded in plagioclase phenocrysts of quaternary volcanics in SE Bam (SE Iran). **Iranian Journal of Earth Sciences**, 11(3), 2019a. p. 215-225.
- YAZDI, A.; SHAHHOSINI, E.; DABIRI, R.; ABEDZADEH, H. Magmatic Differentiation Evidences And Source Characteristics Using Mineral Chemistry In The Torud Intrusion (Northern Iran), **Revista GeoAraguaia**, 9(2), 2019b. p. 6-21

ZAMANI, N.; LOTFI, M.; POURKERMANI, M. Mineralization and related structural-chemical controls by using Remote Sensing studies at chah khaton in Muteh auriferous mine area (Isfahan province Iran), 2020